Binding Energy of Hydrogenic Impurity in GaAs-$Al_xGa_{1-x}As$ Quantum Dots with Different Parameter Combinations

Cheng-Ying Hsieh

德育醫護管理專科學校

Deh Yu College of Nursing and Management, Keelung , Taiwan 204, ROC

Abstract

The low lying state binding energies of hydrogenic impurity located at the center of a GaAs-$Al_xGa_{1-x}As$-$Al_yGa_{1-y}As$ multi-layer quantum dot (MLQD) are calculated with different effective mass and dielectric constant parameter combinations. The MLQD consists of a spherical core (GaAs) and a coated spherical shell($Al_xGa_{1-x}As$). The whole dot is embedded inside a bulk material ($Al_yGa_{1-y}As$). The eigenfunctions of the impurity can be expressed in terms of Whittaker functions and Coulomb wave functions. The ground state and low lying state binding energies are expressed in terms of the dot radius, core radius, and concentration of Al with different parameter combinations. Our result shows the low lying state binding energies is approximate for low concentration of Al and large dot radius. As the concentration of Al increases the difference of binding energy increases. We must consider the difference of the effective mass and dielectric constant between the GaAs and $Al_xGa_{1-x}As$ region for the small dot radius calculations. Our results also show the effective mass is more important than dielectric constant for low lying state binding energy.

PACS Number:63.20.Kr;71.38.+i

1. Introduction

The development and improvement of semiconductor growth techniques such as chemical vapor deposition (CVD), liquid-phase epitaxy (LPE) and molecular beam epitaxy (MBE), have led to the possibility of controlling material composition and of incorporating impurity on the electronic de Broglie scale[1-5]. Impurity states in various confined systems, such as quantum-well wires (QWWs) and quantum dots (QDs), have been a subject of extensive investigations in basic and applied research. The GaAs- $Al_xGa_{1-x}As$ heterostructure system is potentially useful material for high-speed digital, high-frequency microwave, and electro-optic device applications[6].

Understanding the impurity states in the confined system is an important problem in the semiconductor physics. Since Bastard's[7] pioneer works in the study of the binding energy of a hydrogenic impurity within an infinite potential-well structure, many theoretical works have been devoted to the study of the properties of impurity states in various confining systems. The binding energy of the ground state of a hydrogenic impurity E_b in D dimensions is given by[8] $E_b=[2/(D-1)]^2$ Ry, where Ry is the effective Rydberg. In the 2-D case, the binding energy increases four times relative to the 3-D case, while in the 1-D case the increases is infinite. Bryant[9-10] improved the model calculation by assuming a finite barrier for the confining potential with the impurity on and off the axis of cylinder wire. The binding energies for the bound states of hydrogenic impurity in a quantum-well wire of GaAs-$Ga_{1-x}Al_xAs$ have been found to be 2-3 times larger than those of in comparable 2-D wells. In the calculation of the hydrogenic impurity states, a variational principle with a trial wave function which takes into account the confinement of the carriers in the quantum-well wire or the quantum dot was usually employed[9-23]. All of the calculations have shown that the binding energy of the impurity atom in a quantum well depends prominently on the barrier height V_0 and the well size. The physical properties of electrons in quantum dots are very different from those in the bulk. As a consequence of the confinement, energy levels are discrete. The existence of these atomic-like state may be utilized in future laser where laser properties can be tailored by proper choices of well and

barrier materials as well as sizes and shapes of the QDs. The change in impurity binding energies due to confinement effect has been observed in photoluminescence[24-27] and Raman-scattering[28,29] experiments on the impurities in the quantum wells.

The study of the impurity states in quantum dots is of physics interest because specific properties of the impurity in lower-dimensional structures can be achieved easily by varying the radius of the quantum dot. The properties of an impurity atom in a quantum dot may appear to be unaffected by the boundary when the radius is very large. For an impurity in a QD with infinite confining potential, as the radius is reduced, the electron can move only in a smaller space and spends closer to the impurity ion. However, spatial confinement will cause the kinetic energy of the electron to increase due to the uncertainty principle and eventually may make the electron to overcome the attractive potential. Therefore, the total energy of the impurity may change from negative to positive for certain dot radius and finally diverges to infinity as the radius approaches zero. Moreover, the effective strength of the Coulomb interaction between the electron and the impurity atom depends on the geometric dimension of the system and is enhanced as the size of the system is reduced. Thus, the effective strength of the Coulomb interaction in QDs can be adjusted by varying the dot radius. On the contrary, dramatic changes in the binding energies may serve as a clear signal for changes in the effective dimension of QDs.

Our system is constructed as a core dot made of GaAs surrounded by a shell of $Al_xGa_{1-x}As$ and then embedded in the bulk of $Al_yGa_{1-y}As$. The polarization and image charge effects [30-31] can be significant if there is a large dielectric discontinuity between the dot and the surrounding medium. However, this is not the case for the GaAs-$Al_xGa_{1-x}As$ quantum system; therefore we ignore such effects. The barrier height between GaAs and $Al_xGa_{1-x}As$ can be obtained from a fixed ratio Q=0.7 of the band-gap discontinuity[6] $\Delta E_g = 1.247x$ eV for 0 x 0.45 and $\Delta E_g = 0.576 + 0.125x + 0.143x^2$ for 0.45 x 1. In this paper, the effective atomic units are used so that all energies are measured in the units of the effective Rydberg(Ry) and all distances are measured

in the units of effective Bohr radius a_0^*. The Ry and a_0^*. can be determined by $\frac{e^4}{2\ 2\ 2}$ and $\frac{\varepsilon\hbar^2}{e^2}$, where μ and ε are, respectively, the electronic effective mass and the dielectric constant of GaAs material and equal to $0.067m_e$ and 13.18. Then the Ry and a_0^*. are equal to 5.2 meV and 104 ^{o}, respectively. The electronic effective mass and the dielectric constant of $Al_xGa_{1-x}As$ equal to $(0.067+0.083x)m_e$ and 13.18 $3.12x^6$.

Formerly, the calculations are using the effective mass approximation for small size confining system. In this work we calculate the ground state and the low lying state binding energy of the hydrogenic impurity located at the center of the multi-layer quantum dot with five combination for different effective mass and dielectric constant.

2. Theory

A. Hydrogenic impurity confined in the MLQD

Consider a hydrogenic impurity located at the center of a multi-layer spherical dot confined by spherical potential wells. The confining potential V_1 is assumed to be zero inside the dot (r<a), and V_2 inside the shell(a≦r<b), V_3 outside the shell (r≧b), where a is the core radius and b is the total dot (core plus shell) radius, therefore b-a is the thickness of the shell. According to the effective-mass approximation, the Hamiltonian of the system can be written as

$$H=-\frac{\hbar^2}{2}\nabla^2-\frac{e^2}{\varepsilon r}+V(r)$$

where

$$V(r)=\begin{cases}0\ ,if\ r<a\\ V_2\ ,if\ a\le r<b\\ V_3\ ,if\ r\ge b\end{cases}$$

and V(r) is the confining potential, μ and ε are the electronic effective mass and the dielectric constant of the material. The Schrödinger equation expressed in spherical coordinates (r, θ, φ)

$$H\Psi(r,\theta,\varphi)=E\Psi(r,\theta,\varphi) \tag{1}$$

can be written as:

$$-\frac{\hbar^2}{2\mu}\left[\frac{\partial^2}{\partial r^2}+\frac{2}{r}\frac{\partial}{\partial r}+\frac{1}{r^2\sin\theta}\frac{\partial}{\partial\theta}\left(\sin\theta\frac{\partial}{\partial\theta}\right)+\frac{1}{r^2\sin^2\theta}\frac{\partial^2}{\partial\varphi^2}\right]\Psi-\frac{e^2}{\varepsilon r}\Psi+V(r)\Psi=E\Psi \tag{2}$$

Separate $\Psi(r,\theta,\varphi)$ into a product of three terms $R(r)\Theta(\theta)\Phi(\varphi)$. Where $\Theta(\theta)$ can be expressed in terms of the associated Legendre polynomial, and $\Phi(\varphi)=e^{im\varphi}$, m=0, ±1, ±2.... The equation for the radial part R(r) can be obtained as follows:

$$-\frac{\hbar^2}{2\mu}\left[\frac{\partial^2}{\partial r^2}+\frac{2}{r}\frac{\partial}{\partial r}-\frac{L(L+1)}{r^2}\right]R(r)-\frac{e^2}{\varepsilon r}R(r)+V(r)R(r)=ER(r) \tag{3}$$

This equation can be solved in two different situations:

(I). For r<a , V(r)=0,

Eq. (3) can be rewritten as

$$-\frac{\hbar^2}{2\mu}\left[\frac{\partial^2}{\partial r^2}+\frac{2}{r}\frac{\partial}{\partial r}-\frac{L(L+1)}{r^2}\right]R(r)-\frac{e^2}{\varepsilon r}R(r)=ER(r) \tag{4}$$

As the electron is confined inside the core dot, the existence of positive energy bound states is possible, therefore, solutions of the Schrödinger equation can be studied in two regions:

(a). For negative-energy, E<0.

Define $\alpha_{1a}^2=-\frac{8\mu E}{\hbar^2}>0$, $\xi=\alpha_{1a}r$ and $\lambda_1=\frac{2\mu e^2}{\varepsilon\hbar^2\alpha_{1a}}$, then Eq. (4) can be expressed as:

$$\frac{\partial^2 R}{\partial\xi^2}+\frac{2}{\xi}\frac{\partial R}{\partial\xi}+\left[-\frac{1}{4}+\frac{\lambda_1}{\xi}-\frac{L(L+1)}{\xi^2}\right]R=0 \tag{5}$$

If we further write $R(\xi)=\xi^{-1}W(\xi)$, then Eq. (5) becomes

$$\frac{\partial^2 W}{\partial \xi^2}+\left[-\frac{1}{4}+\frac{\lambda_1}{\xi}+\frac{\frac{1}{4}-(L+\frac{1}{2})^2}{\xi^2}\right]W=0 \qquad (6)$$

Eq. (6) is the Whittaker equation [32,33] which has two linearly independent solutions :

$$W_{\lambda_1,L}(\xi)=e^{-\frac{\xi}{2}}\xi^{L+1}\Phi(L+1-\lambda_1,2L+2,\xi) \qquad (7a)$$

or

$$W_{\lambda_1,-L}(\xi)=e^{-\frac{\xi}{2}}\xi^{-L+1}\Phi(-L+1-\lambda_1,-2L+2,\xi) \qquad (7b)$$

where Φ is the confluent hypergeometric function

$$\Phi(a,b,x)=1+\frac{a}{b}\frac{x}{1}+\frac{a(a+1)}{b(b+1)}\frac{x^2}{2!}+\ldots+\frac{a(a+1)\ldots(a+k)}{b(b+1)\ldots(b+k)}\frac{x^k}{k!}+\ldots$$

$$=\sum_{k=0}^{\infty}\frac{(a)_k}{(b)_k}\frac{x^k}{k!}$$

The solution of Eq. (5) can be expressed as:

$$R(\xi)=\xi^{-1}W_{\lambda_1,L}(\xi)=e^{-\frac{\xi}{2}}\xi^{L}\Phi(L+1-\lambda_1,2L+2,\xi) \qquad (8a)$$

or

$$R(\xi)=\xi^{-1}W_{\lambda_1,-L}(\xi)=e^{-\frac{\xi}{2}}\xi^{-L}\Phi(-L+1-\lambda_1,-2L+2,\xi) \qquad (8b)$$

Since the wave function has to be finite everywhere, the solution of the radial part in the r<a region can be expressed as:

$$R_1(\alpha_{1a}r)=C_{1a}e^{-\frac{\alpha_{1a}r}{2}}(\alpha_{1a}r)^{L}\Phi(L+1-\lambda_1,2L+2,\alpha_{1a}r) \qquad (9)$$

where C_{1a} is the normalization constant.

(b). For positive-energy, E>0.

Define $\alpha_{1b}^2 = \frac{2\mu E}{\hbar^2} > 0$, $\xi = \alpha_{1b} r$ and $\beta_1 = -\frac{\mu e^2}{\varepsilon \hbar^2 \alpha_{1b}}$, then Eq. (4) can be expressed as:

$$\frac{\partial^2 R}{\partial \xi^2} + \frac{2}{\xi}\frac{\partial R}{\partial \xi} + \left[1 - \frac{2\beta_1}{\xi} - \frac{L(L+1)}{\xi^2}\right] R = 0 \qquad (10)$$

If we further write $R(\xi) = \xi^{-1} F(\xi)$, then Eq. (10) becomes

$$\frac{\partial^2 F}{\partial \xi^2} + \left[1 - \frac{2\beta_1}{\xi} - \frac{L(L+1)}{\xi^2}\right] F = 0 \qquad (11)$$

Eq. (11) is the Coulomb wave equation[34] which has two linearly independent solutions $F_{\beta_1,L}(\xi)$ and $G_{\beta_1,L}(\xi)$, where

$$F_{\beta_1,L}(\xi) = \xi^{L+1} \Phi_{\beta_1,L}(\xi)., \qquad (12a)$$

$$G_{\beta_1,L}(\xi) = F_{\beta_1,L}(\xi)\left[\ln(2\xi) + \frac{q_L(\beta_1)}{p_L(\beta_1)}\right] + \theta_{\beta_1,L}(\xi) \qquad (12b)$$

and

$$\Phi_{\beta_1,L}(\xi) = \sum_{k=L+1}^{\infty} A_k^L(\beta_1)\xi^{k-L-1}$$

The recurrence relation can be expressed as:

$$A_{L+1}^L(\beta_1) = 1$$

$$A_{L+2}^L(\beta_1) = \frac{\beta_1}{L+1}$$

$$A_k^L(\beta_1) = \frac{2\beta_1 A_{k-1}^L(\beta_1) - A_{k-2}^L(\beta_1)}{(k+L)(k-L-1)} \quad for\ k > L+2$$

$G_{\beta_1,L}(\xi)$ is singular at ξ=0, hence the wave function of the radial part in the region E>0 can be expressed as

$$R_1(\alpha_{1b} r) = C_{1b} \sum_{k=L+1}^{\infty} A_k^L(\beta_1)(\alpha_{1b} r)^{k-1} \qquad (13)$$

where C_{1b} is the normalization constant.

(c). For zero energy E=0.

Substituting E=0 into Eq. (4) , one obtains:

$$r^2\frac{\partial^2 R(r)}{\partial r^2}+2r\frac{\partial R(r)}{\partial r}+\left[-L(L+1)+\frac{2\mu e^2}{\varepsilon\hbar^2}r\right]R(r)=0 \tag{14}$$

Comparing with the modified Bessel equation

$$r^2\frac{\partial^2 u(r)}{\partial r^2}+(1-2\omega)r\frac{\partial u(r)}{\partial r}+(\omega^2-\nu^2\gamma^2+\alpha^2\gamma^2r^{2\gamma})u(r)=0 \tag{15}$$

If we set ω=-1/2, γ=1/2, ν=2L+1, and $\alpha_{1c}^2=\frac{8\mu e^2}{\varepsilon\hbar^2}$, then the solution of Eq. (15) can be expressed as :

$$u(\alpha_{1c}r)=r^{\omega}\left[C_{1c}J_{\nu}(\alpha_{1c}r^{\gamma})+C_{1c}N_{\nu}(\alpha_{1c}r^{\gamma})\right]$$

where $J_{\nu}(\alpha_{1c}r^{\gamma})$ is Bessel function and $N_{\nu}(\alpha_{1c}r^{\gamma})$ is Neumann function. Since the radial function must be finite for L=0, therefore, the wave function of radial part can be written as

$$R_1(\alpha_{1c}r)=C_{1c}r^{-\frac{1}{2}}J_{2L+1}(\sqrt{\frac{8\mu e^2}{\varepsilon\hbar^2}}r^{\frac{1}{2}}) \tag{16}$$

(Ⅱ). For $a\leqq r<b$, $V(r)=V_2$

The differential equation for the radial part R(r) can be expressed as:

$$-\frac{\hbar^2}{2\mu}\left[\frac{\partial^2}{\partial r^2}+\frac{2}{r}\frac{\partial}{\partial r}-\frac{L(L+1)}{r^2}\right]R(r)-\frac{e^2}{\varepsilon r}R(r)+V_2R(r)=ER(r) \tag{17}$$

Define $\alpha_2^2=-\frac{8\mu(E-V_2)}{\hbar^2}>0$, $\xi=\alpha_2 r$, $\lambda_2=\frac{2\mu e^2}{\varepsilon\hbar^2\alpha_2}$ and $R(\xi)=\xi^{-1}W(\xi)$, then Eq. (17) can be rewritten as:

$$\frac{\partial^2 W}{\partial\xi^2}+\left[-\frac{1}{4}+\frac{\lambda_2}{\xi}+\frac{\frac{1}{4}-(L+\frac{1}{2})^2}{\xi^2}\right]W=0 \tag{18}$$

This is the Whittaker equation. Thus, the solution can be written as:

$$R_2(\alpha_2r)=C_{21}e^{-\frac{\alpha_2r}{2}}(\alpha_2r)^L\Phi(L+1-\lambda_2,2L+2,\alpha_2r)$$

$$+C_{22}e^{-\frac{\alpha_2r}{2}}(\alpha_2r)^L\{\Phi(L+1-\lambda_2,2L+2,\alpha_2r)\ln(\alpha_2r)$$

$$+\sum_{k=0}^{\infty}\frac{(L+1-\lambda_2)_k}{(2L+2)_k}\frac{(\alpha_2 r)^k}{k!}\times[\phi(L+1-\lambda_2+k)-\phi(2L+2+k)-\phi(1+k)]+$$

$$+\frac{\Gamma(2L+1)\Gamma(2L+2)\Gamma(-L-\lambda_2)(-1)^{2L+2}}{\Gamma(L+1-\lambda_2)}\times\sum_{k=0}^{2L}\frac{(-L-\lambda_2)_k}{(-2L)_k}\frac{(\alpha_2 r)^{k-2L-1}}{k!}\Bigg\} \qquad (19)$$

where C_{21}, C_{22} are normalization constants.

(Ⅲ). For $r \geqq b$, $V(r)=V_3$

The differential equation for the radial part R(r) can be expressed as:

$$-\frac{\hbar^2}{2\mu}\left[\frac{\partial^2}{\partial r^2}+\frac{2}{r}\frac{\partial}{\partial r}-\frac{L(L+1)}{r^2}\right]R(r)-\frac{e^2}{\varepsilon r}R(r)+V_3R(r)=ER(r) \qquad (20)$$

Define $\alpha_3^2=-\frac{8\mu(E-V_3)}{\hbar^2}>0$, $\xi=\alpha_3 r$, $\lambda_3=\frac{2\mu e^2}{\varepsilon\hbar^2\alpha_3}$, and $R(\xi)=\xi^{-1}W(\xi)$, then Eq. (20) becomes

$$\frac{\partial^2 W}{\partial\xi^2}+\left[-\frac{1}{4}+\frac{\lambda_3}{\xi}+\frac{\frac{1}{4}-(L+\frac{1}{2})^2}{\xi^2}\right]W=0 \qquad (21)$$

This is the Whittaker equation. The Whittaker functions expressed in Eq. (7a) and Eq. (7b) are not well behaved as ξ becomes very large, we thus turn to use the integral representation of Whittaker function

$$W_{\lambda_3,L}(\xi)=C_3e^{-\frac{\xi}{2}}\xi^{\lambda_3}\int_0^{\infty}e^{-t}t^{-\lambda_3+L}(1+\frac{t}{\xi})^{\lambda_3+L}dt \qquad (22)$$

in our calculation. Hence the radial part wave function in the r>b region can be written as

$$R_3(\alpha_3 r)=C_3e^{-\frac{\alpha_3 r}{2}}(\alpha_3 r)^{\lambda_3-1}\int_0^{\infty}e^{-t}t^{-\lambda_3+L}(1+\frac{t}{\alpha_3 r})^{\lambda_3+L}dt \qquad (23)$$

The boundary conditions require:

$$\frac{R_1'(\alpha_1 a)}{R_1(\alpha_1 a)}=\frac{R_2'(\alpha_2 a)}{R_2(\alpha_2 a)} \qquad (24)$$

$$\frac{R_2'(\alpha_2 b)}{R_2(\alpha_2 b)} = \frac{R_3'(\alpha_3 b)}{R_3(\alpha_3 b)} \tag{25}$$

Using above two equations, one can obtain the eigenvalue E.

B. electron confined in the MLQD

The Hamiltonian of an electron confined in the MLQD can be written as:

$$H = -\frac{\hbar^2}{2\mu}\nabla^2 + V(r) \tag{26}$$

where

$$V(r) = \begin{cases} 0 \ , if\ r < a \\ V_2 \ , if\ a \le r < b \\ V_3 \ , if\ r \ge b \end{cases}$$

Schrödinger equation for the radial part R(r) can be expressed in spherical coordinate as:

$$r^2 \frac{\partial^2 R(r)}{\partial r^2} + 2r \frac{\partial R(r)}{\partial r} + \left[-L(L+1) - \frac{2\mu V(r)}{\hbar^2} r^2 \right] R(r) = -\frac{2\mu}{\hbar^2} E r^2 R(r) \tag{27}$$

(I). For r<a , V(r)=0, the Eq. (27) can be written as

$$r^2 \frac{\partial^2 R(r)}{\partial r^2} + 2r \frac{\partial R(r)}{\partial r} + \left[-L(L+1) + \frac{2\mu E}{\hbar^2} r^2 \right] R(r) = 0 \tag{28}$$

Comparing with the modified Bessel equation (Eq. (15)), the wave function of the radial part can be expressed as

$$R_1(r) = C_1 r^{-\frac{1}{2}} J_{L+\frac{1}{2}}\left(\sqrt{\frac{2\mu E}{\hbar^2}} r\right) \tag{29}$$

(II). For a≦r<b, $V(r)=V_2$

Set $\alpha_2^2 = -\frac{8\mu(E - V_2)}{\hbar^2} > 0$, $\xi = \alpha_2 r$, and $R(\xi) = \xi^{-1} W(\xi)$. Then Eq. (27) becomes

$$\frac{\partial^2 W}{\partial \xi^2}+\left[-\frac{1}{4}+\frac{\frac{1}{4}-(L+\frac{1}{2})^2}{\xi^2}\right]W=0 \qquad (30)$$

This is the Whittaker equation. Thus, the solution of the system can be written as

$$R_2(\alpha_2 r)=C_{21}e^{-\frac{\alpha_2 r}{2}}(\alpha_2 r)^L\Phi(L+1,2L+2,\alpha_2 r)+C_{22}e^{-\frac{\alpha_2 r}{2}}(\alpha_2 r)^{-L-1}\Phi(-L,-2L,\alpha_2 r) \qquad (31)$$

(Ⅲ). For r≧b , V(r)=V_3. Let $\alpha_3^2=-\frac{8\mu(E-V_3)}{\hbar^2}>0$, $\xi=\alpha_3 r$, and R(ξ)= ξ^{-1}W(ξ).

Then Eq. (27) becomes

$$\frac{\partial^2 W}{\partial \xi^2}+\left[-\frac{1}{4}+\frac{\frac{1}{4}-(L+\frac{1}{2})^2}{\xi^2}\right]W=0 \qquad (32)$$

which is the Whittaker equation, and the solution of the system can be written as

$$R_3(\alpha_3 r)=C_3 e^{-\frac{\alpha_3 r}{2}}(\alpha_3 r)^{-1}\int_0^{\infty}e^{-t}t^L(1+\frac{t}{\alpha_3 r})^L dt \qquad (33)$$

Using boundary conditions

$$\frac{R_1'(\alpha_1 a)}{R_1(\alpha_1 a)}=\frac{R_2'(\alpha_2 a)}{R_2(\alpha_2 a)} \qquad (34)$$

$$\frac{R_2'(\alpha_2 b)}{R_2(\alpha_2 b)}=\frac{R_3'(\alpha_3 b)}{R_3(\alpha_3 b)} \qquad (35)$$

one can obtain the eigenvalue E.

3. Results and discussions

The binding energy E_b of the impurity is defined as the difference between the electron energy with and without the binding of the impurity atom[9-11, 19-23], i.e.

$$E_b=E_e-E_i$$

where E_i and E_e represent the state energies of electron in multi-layer QD with and without impurity. In this work, we calculate the low lying state binding energy of a hydrogenic impurity located at the center of GaAs-$Al_xGa_{1-x}As$ quantum dot for different

effective-mass and dielectric constant parameter. The effective-mass and dielectric constant are divided into five combinations:

(a). $\mu = m_e$, $\varepsilon = 1$.

(b). $\mu = 0.067m_e$, $\varepsilon = 13.18$.

(c). $\mu = 0.067m_e$, $\varepsilon = 13.18 - 3.12x$.

(d). $\mu = (0.067 + 0.083x)m_e$, $\varepsilon = 13.18$.

(e). $\mu = (0.067 + 0.083x)m_e$, $\varepsilon = 13.18 - 3.12x$.

In our results the cure-a is calculated by the parameter combination-a and the cure-b is calculated by the parameter combination-b, etc. For a single layer quantum dot with very large dot radius, the impurity behaves just like a 3-dimensional free hydrogen atom in the GaAs bulk region, thus its binding energy will approach the 3-dimensional value 1Ry for all different parameter combinations.

Fig. 1 shows the calculated ground state binding energy of a hydrogenic impurity located at the center of a MLQD with x=y as a function of dot radius for $\mu = m_e$, $\varepsilon = 1$ with different alloy compositions: x=0.1, 0.4, 0.8 and 1. Fig. 2 shows the calculated ground state binding energy of a hydrogenic impurity located at the center of a MLQD with x=y as a function of dot radius for $\mu = (0.067 + 0.083x)m_e$, $\varepsilon = 13.18 - 3.12x$ with alloy compositions: x=0.1, 0.4, 0.8 and 1. Comparing Fig. 1 and Fig. 2 the ground state binding energies are similar to large dot radius but different from small dot radius. In Fig. 1 the binding energies all approach 1Ry for different alloy compositions as the dot radius reduces to zero. Fig. 2, the binding energies approach different limit value for different alloy compositions as the dot radius reduces to zero. Since the electron leaks out the quantum dot well to the $Al_xGa_{1-x}As$ region as the dot radius reduces to zero. The limit value of binding energy is dependent on the Al concentration, the limit value increases as the Al concentration increases. In Fig. 1, the approximation doesn't consider the different parameter between GaAs and $Al_xGa_{1-x}As$ region, so all of the limit values approach 1Ry for different alloy concentration.

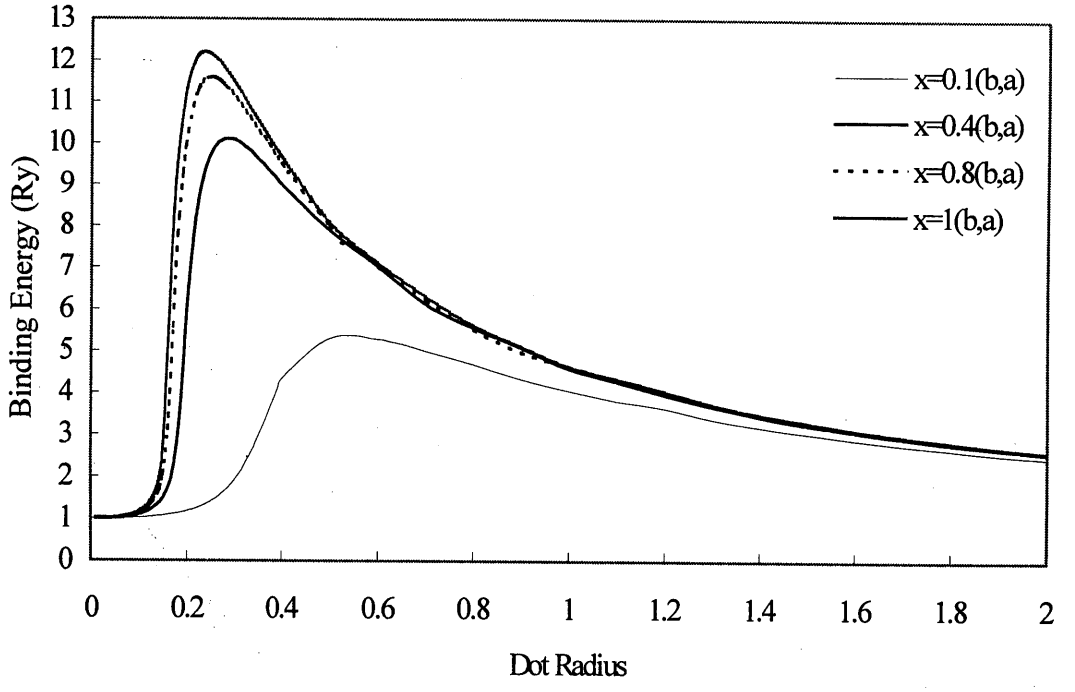

Fig. 1 The ground state binding energy of a hydrogenic impurity in single layer QD as a function of dot radius for $\mu = m_e$, $\varepsilon = 1$ with different alloy compositions: x=0.1, 0.4, 0.8 and 1, respectively.

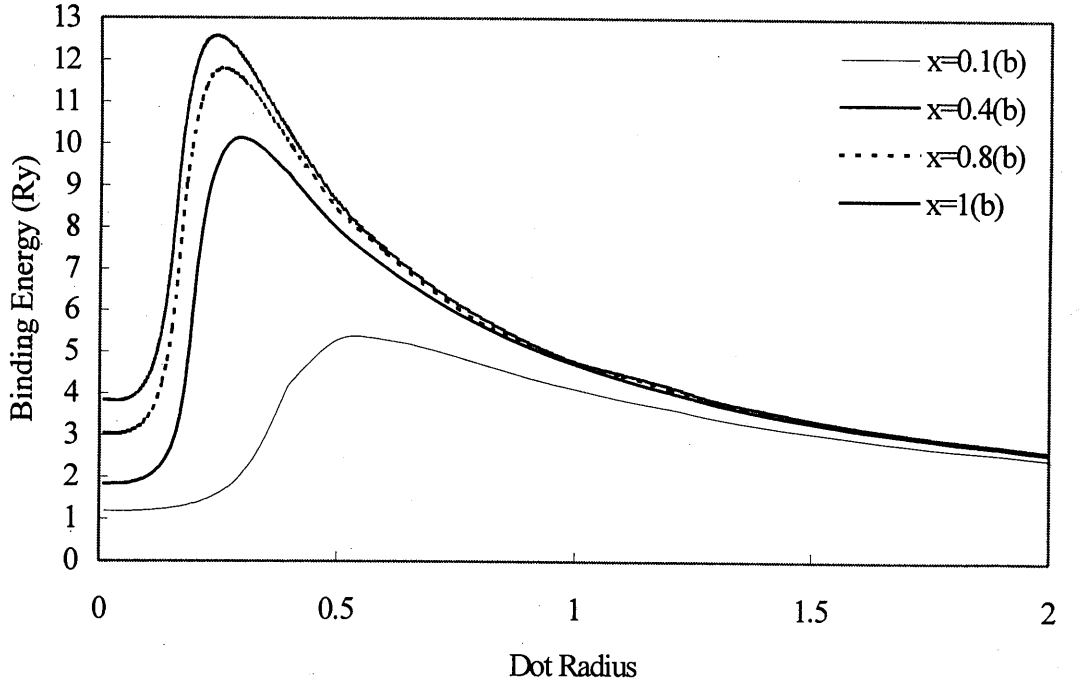

Fig. 2 The ground state binding energy of a hydrogenic impurity in single layer QD as a function of dot radius for $\mu = (0.067 + 0.083x)m_e$, $\varepsilon = 13.18 - 3.12x$ with different alloy compositions: x=0.1, 0.4, 0.8 and 1, respectively.

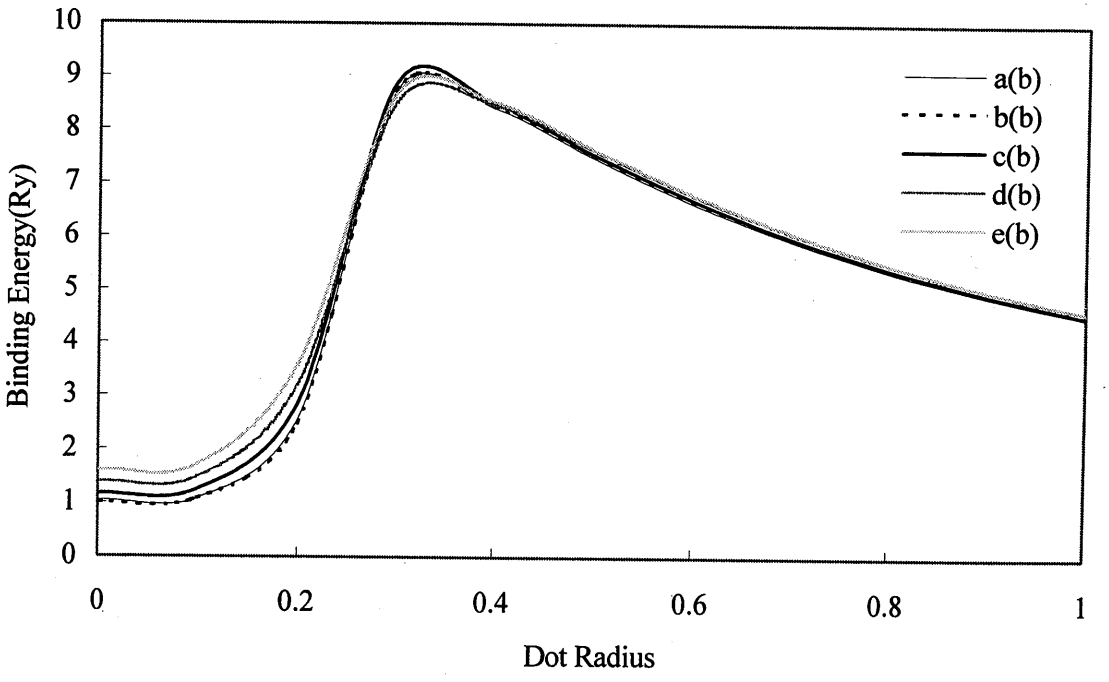

Fig. 3 The ground state binding energy of a hydrogenic impurity in GaAs- $Al_xGa_{1-x}As$ QD as a function of dot radius with concentration of Al x=0.3 for different parameter combinations.

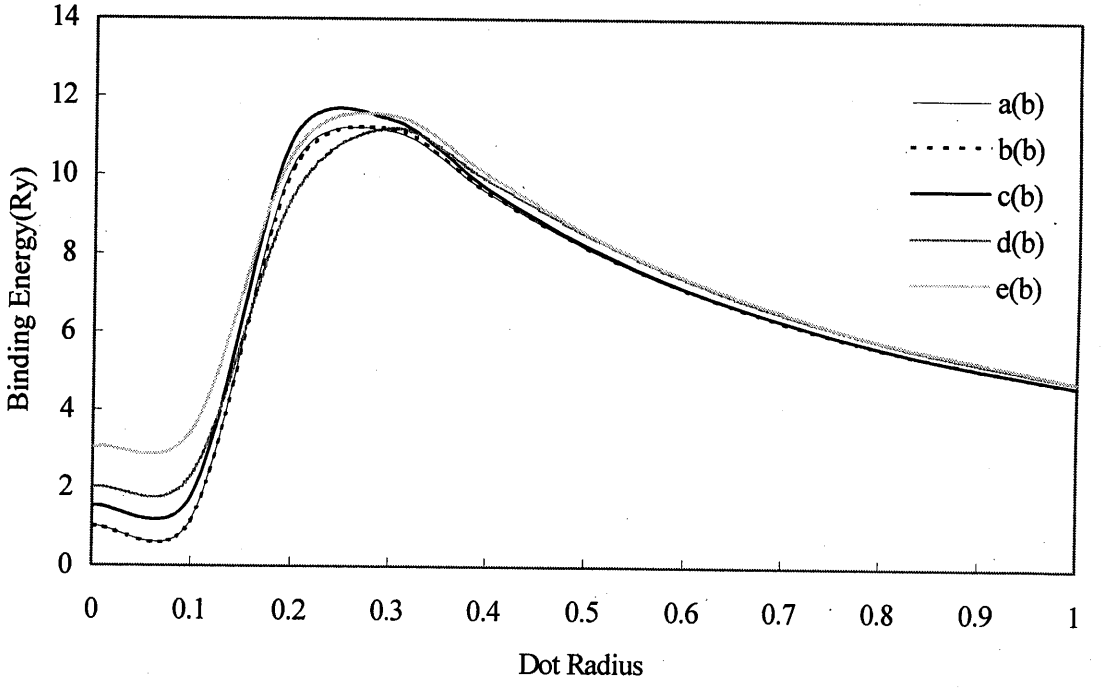

Fig. 4 The ground state binding energy of a hydrogenic impurity in GaAs- $Al_xGa_{1-x}As$ QD as a function of dot radius with concentration of Al x=0.8 for different parameter combinations.

Fig. 3 and Fig. 4 show the ground state binding energy as a function of dot radius for the Al concentration x=0.3 and x=0.8 with five parameter combinations. Comparing the different parameter combination, the binding energy is close for large dot radius and separates farther as the dot radius reduces to zero. Comparing the five combinations of parameter, we can see the effective mass item is more important than the dielectric constant item for the binding energy.

Fig. 5, Fig. 6 and Fig. 7 show the ground state binding energy as a function of Al concentration x with the five parameter combination for dot radius a=0.5 a_0^*, a=1 a_0^* and a=2 a_0^*, respectively. We can see that the binding energy separates farther as the concentration of Al increases in the Figs. 5, 6, 7. Comparing Figs. 5, 6 and 7 we can see the cure-b gets closer to the cure-c and the cure-d gets closer to the cure-e as the dot radius increases.

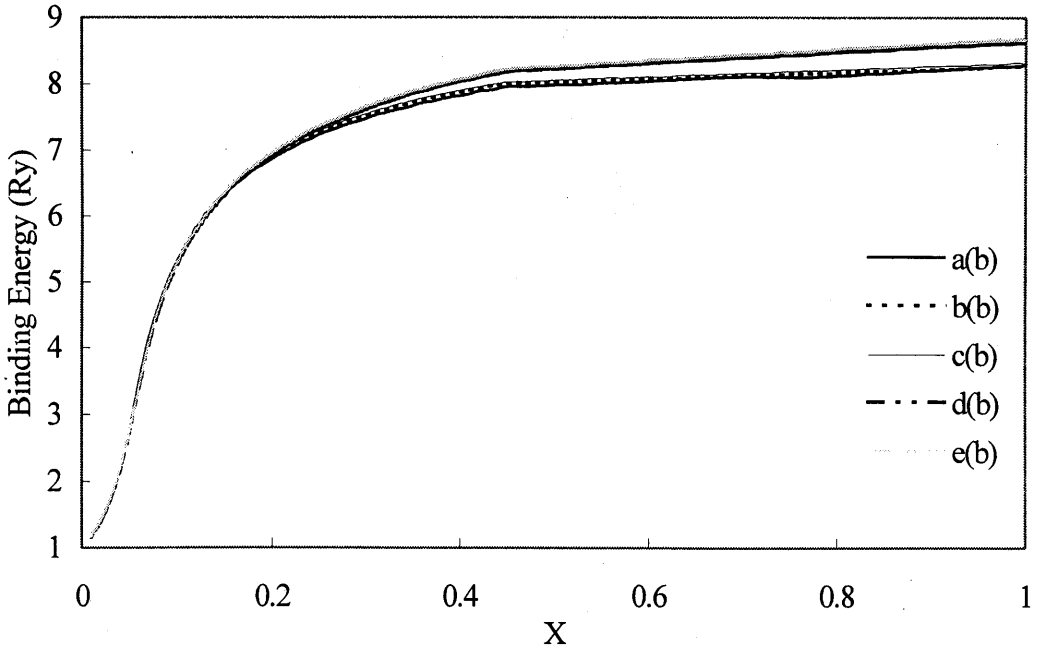

Fig. 5 The ground state binding energy of a hydrogenic impurity in GaAs- $Al_xGa_{1-x}As$ QD as a function of concentration of Al with dot radius a=0.5 a_0^* for different parameter combinations.

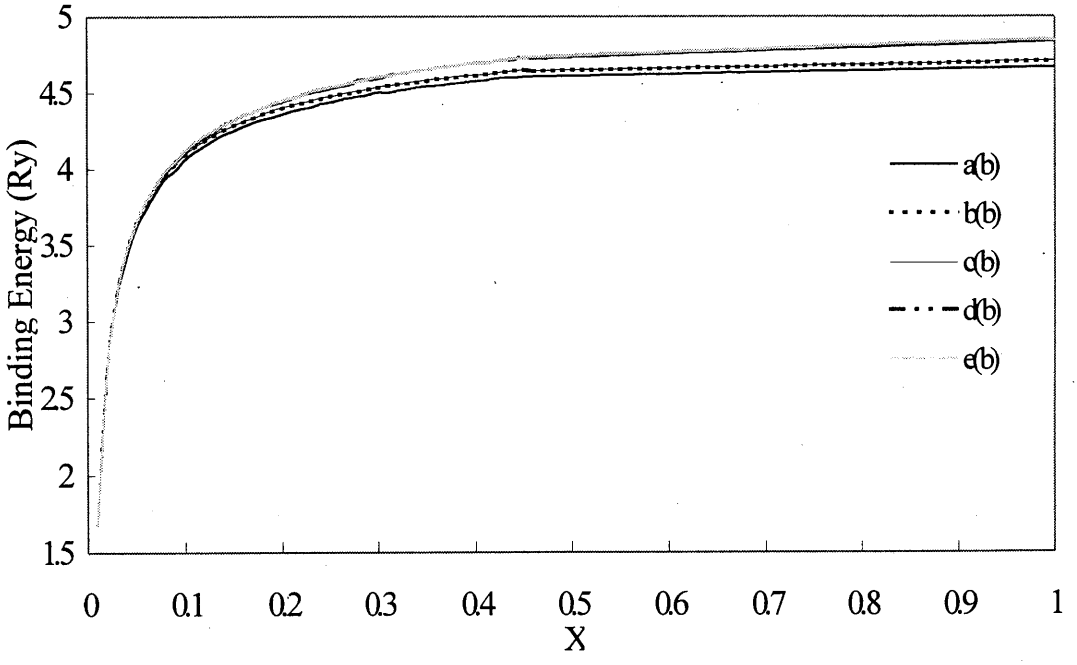

Fig. 6 The ground state binding energy of a hydrogenic impurity in GaAs- $Al_xGa_{1-x}As$ QD as a function of concentration of Al with dot radius a=1 a_0^* for different parameter combinations.

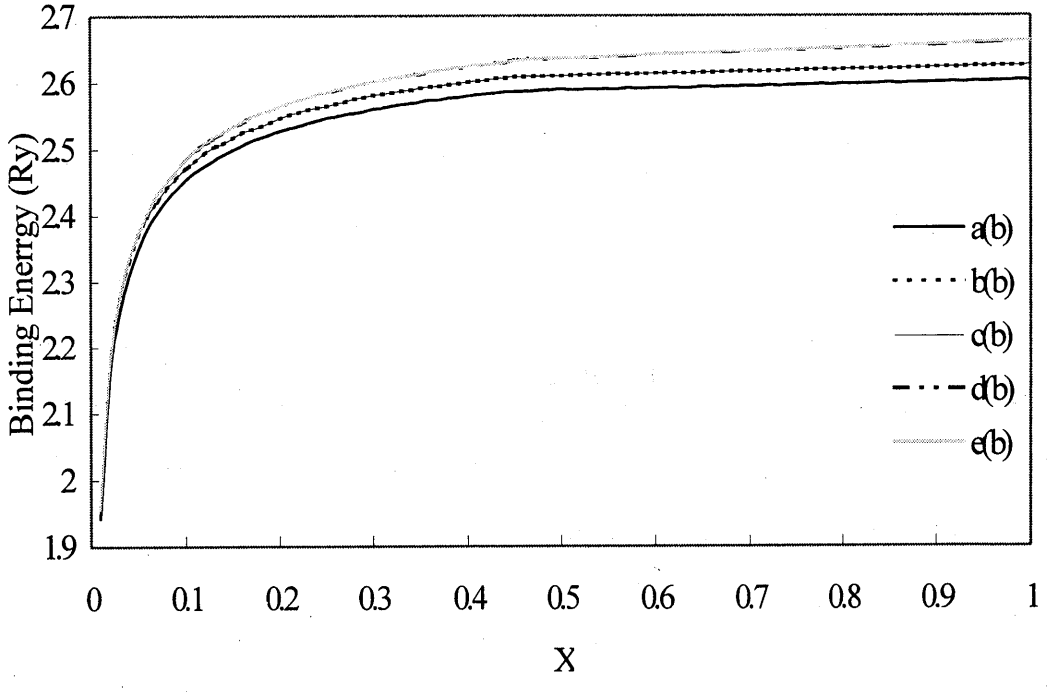

Fig. 7 The ground state binding energy of a hydrogenic impurity in GaAs- $Al_xGa_{1-x}As$ QD as a function of concentration of Al with dot radius a=2 a_0^* for different parameter combinations.

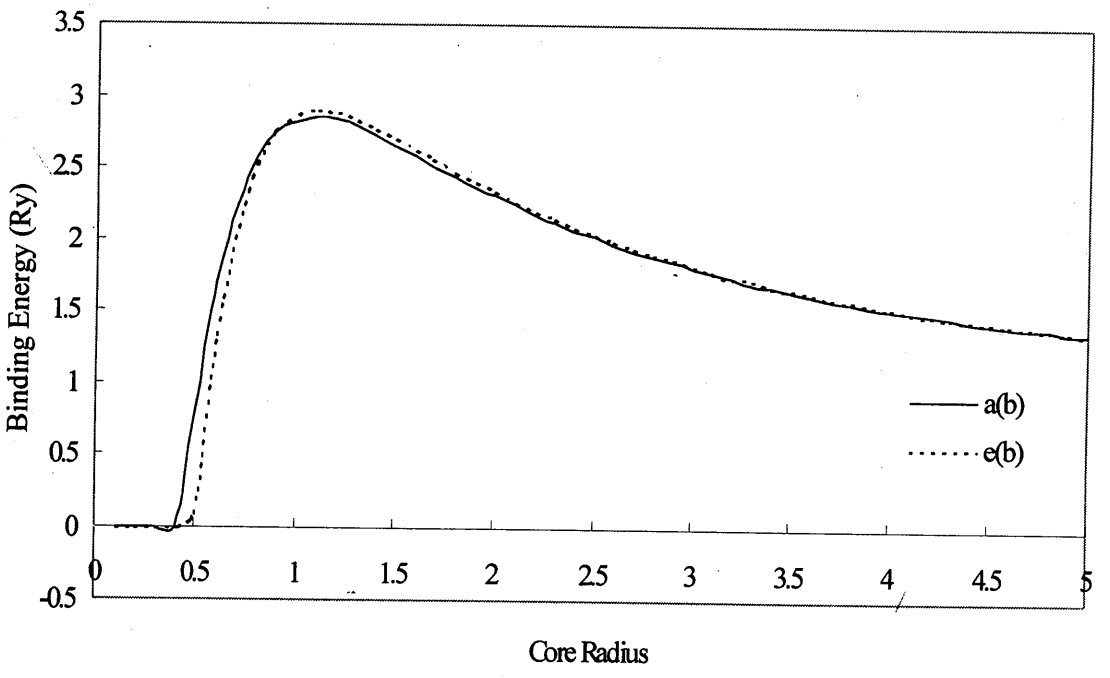

Fig. 8 The ground state binding energy of a hydrogenic impurity in GaAs- $Al_xGa_{1-x}As$ - $Al_yGa_{1-y}As$ multi-layer QD as a function of core radius with x=0.2, y=0.1, and total radius b=24 a_0^* for parameter combinations (a) and (e).

Fig. 8 shows the ground state binding energy of GaAs-$Al_xGa_{1-x}As$-$Al_yGa_{1-y}As$ multi-layer quantum dot as a function of core radius with x=0.2, y=0.1, and the total radius b=24 a_0^* for the parameter combination (a) and (e). We can see the ground state binding energy of MLQD is approximate for low concentration of Al.

Fig. 9 shows the lower lying state binding energy of a hydrogenic impurity in GaAs-$Al_xGa_{1-x}As$ QD as a function of dot radius with the concentration of Al x=0.1 for parameter combination (a) and (e). Our result shows the low lying state binding energy is approximate for low concentration of Al.

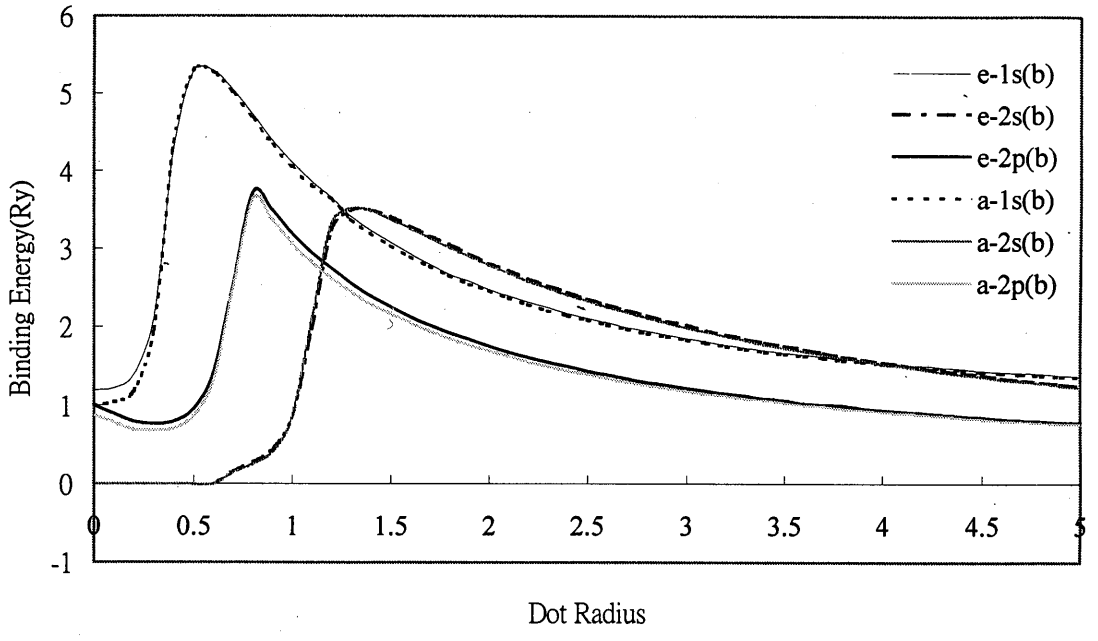

Fig. 9 The low lying state binding energy of a hydrogenic impurity in GaAs- $Al_xGa_{1-x}As$ QD as a function of dot radius with the concentration of Al x=0.1 for parameter combination (a) and (e).

4. Conclusion

We calculate the binding energy of an hydrogenic impurity in a multi-layer QD which consists of a spherical core(GaAs) coating with a spherical shell ($Al_xGa_{1-x}As$) and embedded in a bulk material ($Al_yGa_{1-y}As$) with five parameter combinations. Our result shows the low lying state binding energies is approximate for low concentration of Al and large dot radius. As the concentration of Al increases the difference of binding energy increases. We must consider the difference of the effective mass and dielectric constant between the GaAs and $Al_xGa_{1-x}As$ region for the small dot radius calculations. Our results also show the effective mass is more important than dielectric constant for low lying state binding energy.

5. Acknowledgment

This work was supported by Deh Yu College of Nursing and Management, Taiwan, Republic of China.

6. References

1. T. Fukui, S. Ando, and Y. Tokura Appl. Phys. Lett. **58**, 2018(1991).
2. H. Fang, R. Zeller, and P. J. Stiles Appl. Phys. Lett. **55**, 1433(1989).
3. T. P. Smith III, K. Y. Lee, C. M. Knoedler, J. M. Hong, and D. P. Kern Phys. Rev. B **38**, 2172 (1988).
4. M. A. Reed, J. N. Randall, R. J. Matyi, T. M. Moore, and A. E. Wetsel Phys. Rev. Lett. **60**, 535 (1988).
5. Q. Ye, R. Tsu, and E. H. Hicollian Phys. Rev. B **44**, 1806(1991).
6. S. Adachi, J. Appl. Phys. **58**, R1(1985).
7. G. Bastard, Phys. Rev. B **24**, 4714(1981).
8. X. F. He, Phys. Rev. B **43**, 2063(1991).
9. G. W. Bryant Phys. Rev. B **29**, 6632(1984).
10. G. W. Bryant Phys. Rev. B **31**, 7812(1985).
11. J. W. Brown and H. N. Spector, J. Appl. Phys. **59**, 1179(1986)
12. R. L. Greene and K. K. Bajaj, Solid State Commun. **45**, 825(1983).
13. C. Mailhiot, Y. C. Chang, and T. C. McGill, Phys. Rev. B **26**, 4449(1982).
14. N. P. Montenegro, J. Lopez-Gondar, and L. E. Oliveira Phys. Rev. B **43**, 1824(1991).
15. W. T. Masselink, Y. C. Chang, and H. Morkoc Phys. Rev. B **28**, 7373(1983).
16. S. V. Branis, G. Li, and K. K. Bajaj Phys. Rev. B **47**, 1316(1993).
17. S. V. Nair, L. M. Ramaniah, and K. C. Rustagi Phys. Rev. B **45**, 5969(1992).
18. G. T. Einevoll and Y. C. Chang Phys. Rev. B **40**, 9683(1989).
19. N. P. Montenegro and S. T. P. Merchancano, Phys. Rev. B **46**, 9780(1992).
20. J. L. Zhu, J. H. Zhao, W. H. Duan, and B. L. Gu, Phys. Rev. B **46**, 7546(1992).
21. J. L. Zhu, J. J. Xiong, and B. L. Gu Phys. Rev. B **41**, 6001(1990).
22. J. L. Zhu and X. Chen Phys. Rev. B **50**, 4497(1994).
23. D. S. Chuu, C. M. Hsiao, and W. N. Mei Phys. Rev. B **46**, 3898(1992).
24. R. C. Miller, A. C. Gossard, W. T. Tsang, and O. Munteanu, Phys. Rev. B **29**, 3871(1982)
25. K. Kash, A. Scherer, J. M. Worlock, H. G. Graighead, and M. C. Tamargo Appl. Phys. Lett. **49**, 1043(1986).
26. B. J. Skromme, R. Bhat, and M. A. Koza, Solid State Commun. **66**, 543(1988)

27. H. Temkin, G. J. Dolan, M. B. Panish, and S. N. G. Chu Appl. Phys. Lett. **50**, 413(1987).

28. B. V. Shanabrook, J. Comas, T. A. Perry, and R. Merlin, Phys. Rev. B **29**, 7096(1984)

29. D. Gammon, R. Merlin, W. T. Maselink, H. Morkoc, Phys. Rev. B **33**, 2919(1986)

30. M. Lannoo, C. Delerue and G. Allan Phys. Rev. Lett. **74**, 3415(1995).

31. C. R. Proetto, Phys. Rev. Lett. **76**, 2824(1996).

32. A. Jeffrey, I. Ryzhik, I. Gradshteyn, Yu. Geronimus, and M. Tseytlin Table of Integrals, Series, and Products (Academic Press, New York, 1980)p. 1059.

33. G. Arfken Mathematical Methods for Physicists second edition (Academic Press, New York, 1973)p. 639

34. A. Abramowitz and I. A. Stegun Handbook of Mathematical Function with Formulas, Graphs, and Mathematical Tables, Natl. Bur. Stand. Appl. Math. Series No. 55 (U. S. GPO, Washington, D. C., 1964)p. 538.